FISITA
WORLD CONGRESS

PREDICTIVE HAPTIC DRIVER SUPPORT NEAR VEHICLE'S HANDLING LIMITS

Kazimierz Dokurno[1,2,3], Andrea Michelle Rios Lazcano[2], Xabier Carrera Akutain[2], and Barys Shyrokau[3]

[1] *University of Twente*
Drienerlolaan 5, 7522 NB Enschede, Netherlands (E-mail: k.dokurno@student.utwente.nl)
[2] *Toyota Motor Europe NV/SA*
Hoge Wei 33B, 1930 Zaventem, Belgium (E-mail: {andrea.lazcano, xabier.carrera.akutain}@toyota-europe.com)
[3] *Delft University of Technology*
Mekelweg 2, 2628 CD Delft, The Netherlands (E-mail: b.shyrokau@tudelft.nl)

ABSTRACT: This research presents a novel driver assistance system that anticipates and mitigates understeer by delivering haptic support to the driver via the steering wheel. The proposed system calculates a safe steering envelope using a Model Predictive Control (MPC) framework, considering the saturation limits of the vehicle's front tires. If the predicted driver steering angle violates the safe envelope, haptic feedback is provided through the steering wheel in the form of an increased opposing torque with vibrations. Thus, the system aims to notify drivers of potential understeer and guide them in reducing the steering angle if they exceed the safe steering limits. To evaluate the effectiveness of the proposed support system, a total of 32 drivers participated in a driving simulator experiment at Toyota Motor Europe. The scenario involved an obstacle avoidance maneuver in the middle of a turn at high velocity. Two levels of automation were investigated: 1) haptic support where the additional haptic torque is provided at the steering wheel, and 2) no support which is equivalent to manual steering. The results demonstrate that haptic support has a positive impact on regular drivers, supporting them to mitigate understeer and significantly reducing lane deviation. No significant difference in performance was noted for expert drivers. Novice drivers report significantly reduced mental workload and lower frustration when the haptic support is active. Subjective evaluation indicates strong acceptance of the proposed assistance system.

KEY WORDS: Haptic shared control, model predictive control, human-machine interaction, handling limits, safety envelope.

1. Introduction

Recent developments in sensing, actuation, and computer processing technologies allow the introduction of more enhanced Advanced Driver Assistance Systems (ADAS). This enables the support of the driver in a wider range of conditions and improves driving safety [1]. Despite these advances, statistics still show high rates of accidents caused by unintended lane or road departures, especially during cornering maneuvers [2]. This can be related to excessive vehicle *understeer* when the vehicle speed is too high to negotiate the turn, resulting in an unexpected deviation from the desired path [3][4]. Current state-of-the-art vehicle stability control (VSC) systems can mitigate understeer to some degree through direct yaw control (DYC). Although this approach is effective in aligning the vehicle's heading angle with the turn direction, it relies on differential braking which can saturate the front tires (especially close to the handling limits). This reduces the cornering force and causes the vehicle to follow a wider path than desired.

Different understeer prevention techniques have been proposed that simultaneously aim to limit understeer and improve road holding. Gordon et al. [5] formulated the trade-off between path tracking and yaw rate correction as an optimal control problem. By efficiently using differential braking, the assistance system outperformed classic DYC in minimizing lateral path deviation during cornering. This solution was further improved through the addition of active front steering by Gao et al. [6] and the extension to independent front steering by Fors et al. [7]. However, all these approaches require

prior knowledge of the desired trajectory. If the predicted path deviates substantially from the driver's intention, it can result in driver frustration, loss of trust, and lack of user acceptance [8].

Takahashi et al. [9] proposed a trajectory-agnostic method to understeer mitigation inspired by the driver longitudinal control model developed by Yamakado and Abe [10]. In the study, differential braking is applied proportionally to the lateral jerk, reducing understeer through a combination of deceleration and weight transfer to the front axle. Although this approach does not rely on knowledge of the desired trajectory, it could lead to dangerous situations involving following traffic due to excessive braking.

While the above-mentioned solutions (partially) overrule the driver in emergency situations, another type of systems relies on the concept of shared steering control [11]. These systems promote collaboration such that the assistance system and the driver act together to perform the maneuver successfully. Katzourakis [12] proposed haptic shared control (HSC) as a method for understeer mitigation. The system informs the driver of the handling limits by emphasizing the drop of the self-aligning moment on the steering wheel. This is achieved by inferring the front axle slip angle, which is used to generate haptic torque in case the slip angle is close to the peak lateral slip. The experimental results showed a positive impact of the proposed system on vehicle performance with a reduction in slip angles indicating a better utilization of the front tires. Van Doornik [13] proposed an alternative to Katzourakis' model-based method. Instead of relying on a tire model, direct measurements of the tire

lateral force and the self-aligning moment are used by load-sensing bearings [14]. The ratio between lateral force and self-aligning moment is used to generate haptic feedback which decreases the perceived steering wheel stiffness. Although the drop in self-aligning moment can be considered as an early indicator of tire saturation, the self-aligning moment itself is very sensitive to the vertical tire load, tire-road friction and even the type of tire compounds used [15]. Thus, detecting understeer from the self-aligning moment drop is not robust for dynamic and unknown operating conditions.

Hildebrandt et al. [16] developed a haptic driver understeer assistance which increases the perceived steering torque when understeer is detected by an on-board VSC. The system showed a positive impact on drivers, who used smaller steering inputs near handling limits, resulting in smaller lateral deviation from the lane. However, the system is reactive rather than proactive due to understeer detection by VSC, which relies on the comparison of yaw rate and lateral acceleration with a reference behaviour. This indicates that significant understeer has to happen in order to be detected, informing the driver only after the situation has already become critical.

Hence, there is a lack of systems which include the driver in the control loop and simultaneously predict the approaching handling limits.

This study addresses this gap with an intuitive haptic driver support system with predictive capabilities for understeer mitigation. Haptic torque is used to alert the driver about incoming handling limits and offers guidance for handling the situation in a safer manner. The proposed system adheres to the following principles:

1. the occurrence of understeer is predicted in advance,

2. the driver is part of the control loop at all times,

3. no knowledge of the desired path is required,

4. the system intervenes only when necessary.

Using model predictive control (MPC), this study proposes a controller to predict the future vehicle states and steering input based on a bicycle model with a brush tire model. A safe steering envelope is computed based on the predicted states for the prediction horizon by a low-level controller. In case the predicted steering input violates the safe steering envelope, the low-level controller generates a haptic torque directly on the steering wheel. This alerts the driver about the incoming saturation of the front tires and offers guidance towards a safer steering input.

The remainder of this paper is organized as follows. Section 2 presents the model used to quantify the vehicle dynamics and develop the safe steering envelope, which is subsequently used in Section 3 for the design of the haptic driver support system. The performed driving simulator experiment is presented in Section 4 and the study results are shown in Section 5. Conclusions are drawn in Section 6 along with recommendations for future work.

2. Vehicle Model

The predictive haptic driver support relies on two models. The vehicle model is used to predict the lateral and rotational velocities of the car, while the tire model allows to calculate the forces at the tire-road contact patch.
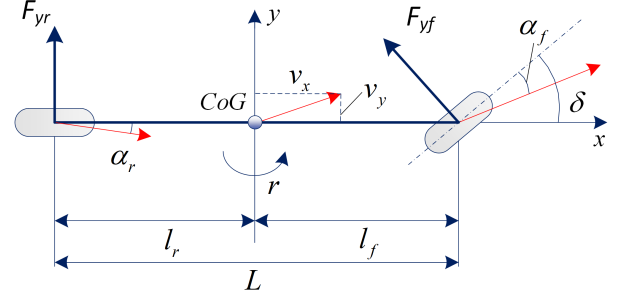

Figure 1. Bicycle model

2.1. Bicycle Model

The vehicle model used is a single-track model with two degrees of freedom [17]. The bicycle model, illustrated in Figure 1, considers the tires on each axle lumped together and assumes a constant longitudinal velocity v_x, no load transfers and no vertical motion of the vehicle. The equations of motion can be written in terms of the front and rear tire forces, F_{yf} and F_{yr}, as

$$\dot{v}_y = \frac{F_{yf} + F_{yr}}{m} - rv_x \,, \tag{1}$$

$$\dot{r} = \frac{l_f F_{yf} - l_r F_{yr}}{I_{zz}} \,, \tag{2}$$

where v_y is the lateral velocity, r is the yaw rate, l_f and l_r are the distances from the center of gravity (CoG) to the front and rear axle, m is the vehicle mass and I_{zz} is the moment of inertia. From kinematics, the equations for the tire slip angles at the front (α_f) and at the rear (α_r) can be found as

$$\alpha_f = \frac{v_y + l_f r}{v_x} - \delta \,, \tag{3}$$

$$\alpha_r = \frac{v_y - l_r r}{v_x} \,, \tag{4}$$

where δ is the road-wheel steer angle.

2.2. Tire Brush Model

In this study, a nonlinear brush model proposed by Fiala [18] has been chosen due to its accurate description of tire behavior up to the tire saturation limits and light complexity ensuring real-time application. An adapted version of the model formulated by Pacejka [15] is used. The model assumes a parabolic pressure distribution at the contact patch, a rigid tire carcass and a constant friction coefficient μ. Given these assumptions, the relation between the lateral tire force $F_{y[f,r]}$ and $\alpha_{[f,r]}$ is described by

$$F_y = \begin{cases} C_\alpha \tan \alpha - \dfrac{C_\alpha^2}{3\mu F_z} |\tan \alpha| \tan \alpha \\ \qquad\qquad + \dfrac{C_\alpha^3}{27\mu^2 F_z^2} \tan^3 \alpha \,, & \text{if } |\alpha| \leq \alpha_{lim} \\ \mu F_z \text{sgn}\alpha \,, & \text{else} \end{cases} \tag{5}$$

where C_α is the tire cornering stiffness, F_z is the normal load and α_{lim} is the slip angle at which the tire has reached the limits of friction, equal to

$$\alpha_{lim} = \tan^{-1} \left(\frac{3\mu F_z}{C_\alpha} \right) \,. \tag{6}$$

2.3. Safe Steering Envelope

Based on the concept of *envelope control* [19], the support system only acts to help the driver maintain the vehicle in a region of operation delimited by safe boundaries, while remaining inactive away from these limits.

Substituting (6) into (3) and isolating δ yields an expression for the upper and lower boundary of the road-wheel angle δ_{lim} at which F_{yf} reaches its peak value, respectively:

$$\delta_{lim}^{+} = \frac{v_y + l_f r}{v_x} + \tan^{-1}\left(\frac{3\mu F_z}{C_\alpha}\right), \tag{7}$$

$$\delta_{lim}^{-} = \frac{v_y + l_f r}{v_x} - \tan^{-1}\left(\frac{3\mu F_z}{C_\alpha}\right). \tag{8}$$

As long as δ remains within the bounds given in (7) and (8), the front tire slip angle will remain under its saturation value.

3. Haptic Support System Design

The goal of the controller is to keep the vehicle within the handling limits, by restricting the road-wheel angle to the boundaries defined in (7) and (8). In order to achieve this objective while keeping the driver in the control loop, the following control architecture is proposed. A high-level MPC controller is designed for predicting the vehicle states and the road-wheel angle over a certain time horizon. These predictions serve as input to the low-level HSC controller which calculates the safe steering envelope for every predicted timestep and subsequently provides haptic feedback on the steering wheel in case the envelope is violated. The overall structure of the predictive haptic driver support system is shown in Figure 2.

3.1. High-level Control

An optimization problem is solved over a receding time horizon, while taking into account modelled vehicle dynamics, constraints, and desired objectives. In this study, the state vector x is defined as $x = [v_y, r, \delta]$ and the control input u is the steering velocity $u = \dot{\delta}$. The goal of the controller is to predict the driver input as closely as possible, without *a priori* knowledge of the path. For short time intervals, the steering velocity can be assumed constant such that the future road-wheel angle is computed by integrating the steering velocity over time. Furthermore, the input $\dot{\delta}$ should not be too large and the resulting δ should not deviate significantly from the initial road-wheel angle at the start of the prediction. These requirements are reflected in the chosen least-squares cost function. The optimization problem that the MPC solves to predict the future vehicle states is formulated as follows:

$$\min_{\dot{\delta}} \quad \sum_{k=1}^{N_p} \left(\left\| \dot{\delta}_k \right\|_{Q_1}^2 + \left\| \dot{\delta}_k - \dot{\delta}_0 \right\|_{Q_2}^2 + \left\| \delta_k - \delta_0 \right\|_{Q_3}^2 \right)$$
$$\text{s.t.} \quad x[k+1] = Ax[k] + Bu[k] + d[k]$$
$$-\frac{\pi}{2} \leq \delta \leq \frac{\pi}{2} \tag{9}$$

In the cost function, δ_0 and $\dot{\delta}_0$ are the initial road-wheel angle and velocity, respectively, and Q_1, Q_2 and Q_3 are the tuning weights. Furthermore, A, B and d are respectively the system matrix, the input matrix and the disturbance input associated with the current state from the discrete state-space vehicle model. The discrete state-space is obtained by discretizing the continuous bicycle model defined in (1) and (2), combined with the slip and tire model defined

in (3), (4), (5) and (6). The constraint on δ reflects the actuation limits of the steering system.

3.2. Low-level Control

From the obtained predictions, the low-level controller calculates the safe steering envelope boundaries for each timestep of the prediction horizon using (7) and (8). If the predicted road-wheel angle exceeds the calculated limits at any point, an error term is generated for that particular timestep as follows:

$$e_k = \begin{cases} \delta_{lim,k}^{-} - \delta_k, & \text{if } \delta_k < \delta_{lim,k}^{-} \\ 0, & \text{if } \delta_{lim,k}^{-} \leq \delta_k \leq \delta_{lim,k}^{+} \\ \delta_{lim,k}^{+} - \delta_k, & \text{if } \delta_{lim,k}^{+} < \delta_k \end{cases} \tag{10}$$

The error of each particular timestep k is multiplied by a decreasing weighting term $(N_p - k + 1)$ in order to assign more importance to imminent errors compared to errors further ahead in the horizon. The weighted sum is scaled by a tuning factor K in order to generate a haptic torque τ_{hap} which is noticeable but can also be overruled by the driver:

$$\tau_{hap} = K \sum_{k=1}^{N_p} (N_p - k + 1)e_k, \tag{11}$$

In addition to the increase in steering torque, torque vibrations τ_{vib} of fixed amplitude A_{vib} and frequency f_{vib} are also added to the steering wheel. These vibrations were perceived as a positive influence on user acceptance during the pilot study. The total support torque τ_s delivered by the system to the steering wheel is equal to $\tau_{hap} + \tau_{vib}$.

3.3. Implementation

The resulting optimization problem in (9) is nonlinear and requires the use of efficient solvers in order to guarantee real-time implementation. For this study, the problem is solved using FORCES PRO NLP solver [20][21], using the real-time variant of the sequential quadratic programming method. The controller has been implemented in MATLAB Simulink, with a sample time of $0.01s$. It was noted that without information about the incoming path, for normal driving conditions, predictions based on the current vehicle state and driver input are only accurate for around $0.5s$. Beyond this time, steering velocity cannot be assumed to be approximately constant anymore and predictions deviate significantly from the actual states. Therefore, a prediction horizon of $0.5s$ was chosen as it results in good prediction accuracy while allowing enough margin for understeer to be detected ahead of time. MPC tuning weights were adjusted to improve the accuracy of the state prediction. The selection of the haptic torque tuning factor K was done during the pilot study with an expert driver to achieve a desired level of control authority. All relevant controller parameters are summarized in Table 1.

Figure 3 illustrates the controller operation during one of the experimental trials described in the next section. The two uppermost plots show the predicted states, $\hat{r}$ and $\hat{v}_y$, coming from the MPC at $t = 38.17s$ for the length of the prediction horizon, until $t = 38.67s$. The predicted steering input $\hat{\delta}$ exceeds the calculated safe steering boundary around the $38.6s$ mark, as shown in the third plot. The support torque τ_s is provided as soon as the limit violation is predicted, as can be seen in the last plot. For reference, the recorded vehicle states and driver input are also shown.
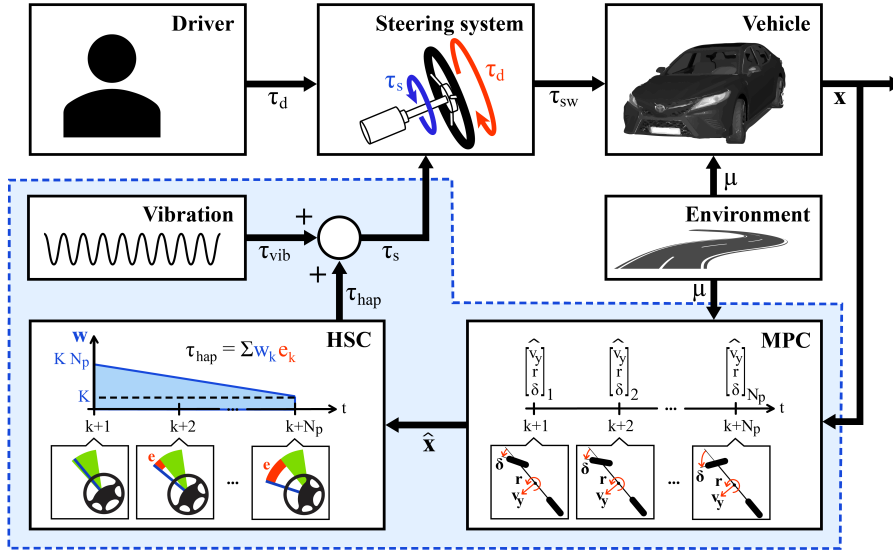
Figure 2. Controller diagram: The MPC predicts the future vehicle states, which are then used to compute the safe steering envelope (in green) for each timestep of the prediction horizon. An error e (in red) is produced if the predicted steering angle leaves the envelope. The generated haptic torque τ_{hap} is equal to the weighted sum of the errors where the weighting function w is linearly decreasing. The total support torque τ_s is equal to the sum of τ_{hap} and τ_{vib}.

Parameter	Description	Value
T_c	controller sample time in s	0.01
N_p	number of timesteps in prediction horizon	50
Q_1	weight on steering velocity	10
Q_2	weight on steering velocity deviation	2000
Q_3	weight on steering angle deviation	0.1
K	haptic torque tuning factor	0.05
A_{vib}	haptic vibration amplitude in Nm	0.5
f_{vib}	haptic vibration frequency in Hz	21

Table 1. Controller parameters

4. Experiment Design

In order to validate the proposed system, a driver-in-the-loop study was performed at Toyota Motor Europe on a high-fidelity driving simulator, which uses a static mock-up of a Toyota production vehicle in front of a $210°$ projection screen. The graphics were rendered with rFpro software based on an IPG CarMaker scenario. The simulator uses a vehicle dynamics model with a proprietary steer-by-wire model and a Toyota production vehicle parametrisation. The control loading system is used to measure the driver's steering input and provide realistic steering feedback during driving [22], alongside the additional torque provided by the haptic support system. The complete setup can be seen in Figure 4.

Two variations of the haptic support system have been investigated:

- *No support*: this case represents manual steering equivalent to a conventional vehicle with electric power assisted steering. There is no additional haptic torque added to the steering wheel. This variation is used as baseline.
- *Haptic support*: in this case, there is additional haptic torque together with vibrations added to the steering wheel when the controller predicts the violation of the safe steering envelope.

4.1. Driving Scenario

The aim of the conducted experiments was to validate the proposed system under naturalistic driving conditions during which the vehicle approaches the limits of handling. A 1km long circuit was designed with straight sections as well as curves with a constant 50m cornering radius. The tire-road friction coefficient μ was set to 0.8. The vehicle velocity was set to 70km/h to recreate a situation in which the vehicle enters a corner with excessive speed and is close to the limits of handling. Similar to the study of Othman et al. [23] on overtaking maneuvers in curves, an obstacle was set to obstruct the right lane on one of the corners. As a consequence, participants are forced to perform an avoidance maneuver in the middle of a turn. This situation is known to cause a large lateral acceleration peak which makes it even more difficult to negotiate the turn. The complete circuit can be seen in Figure 5.

4.2. Participants

In total, 32 participants conducted the experiment, all with a valid driving license. Among them, there were expert test drivers with professional experience in handling limit driving. Prior to conducting the experiment, each participant completed 6 practice runs on the same circuit, but without the obstacle: 3 runs without steering support and 3 runs with the haptic support enabled. This allowed them to become familiar with the driving simulator and the additional haptic torque on the steering wheel. The participants were instructed to remain in the right lane while driving, without using the gas or brake pedal. The practice runs without haptic support have been used to classify between regular and novice drivers. Those who managed to stay within the lane's boundaries were classified as regular drivers (N=15), while those who left the lane were classified as novice drivers (N=12). Expert drivers (N=5) were selected based on their professional qualifications.

From self-reported data, the mean age of an expert driver was 39.4 years (SD = 4.22), with an average driving license possession of
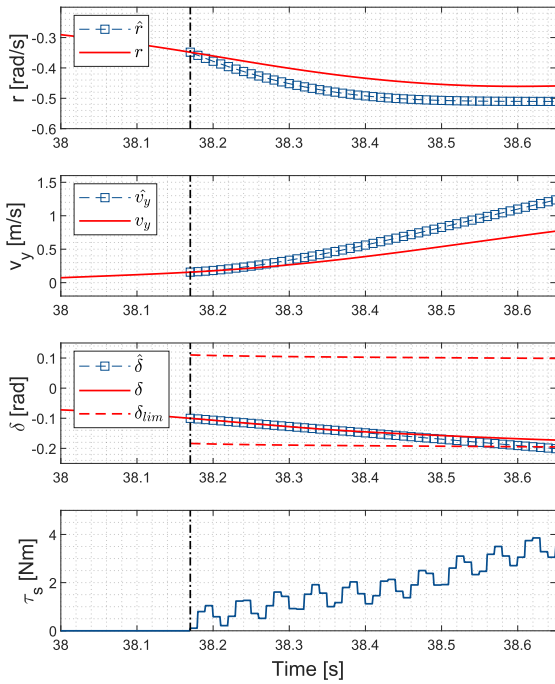
Figure 3. State prediction at $t = 38.17$s during a driver-in-the-loop experimental trial

Figure 4. Driving simulator at Toyota Motor Europe, Belgium

20.8 years (SD = 5.07). The average age of a regular driver was 28.53 years (SD = 7.12) with an average driving license possession of 10.4 years (SD = 7.11). Finally, the average age of a novice driver was 25.33 years (SD = 2.39) with an average driving license possession of 5.51 years (SD = 2.98).

4.3. Experimental Procedure

The experimental trials were performed immediately after the practice session. Each participant was instructed to keep the right lane as much as possible, with the gas and brake pedals deactivated. An obstacle was obstructing the right lane at the 460m mark, right in the middle of a corner. Participants were asked to avoid any obstacle by moving to the left lane and then returning to the right lane as fast as they could. Each test subject performed 6 runs on the circuit: 3 runs with the haptic support and 3 runs without any support. The runs were in random order (Randomised Latin Square
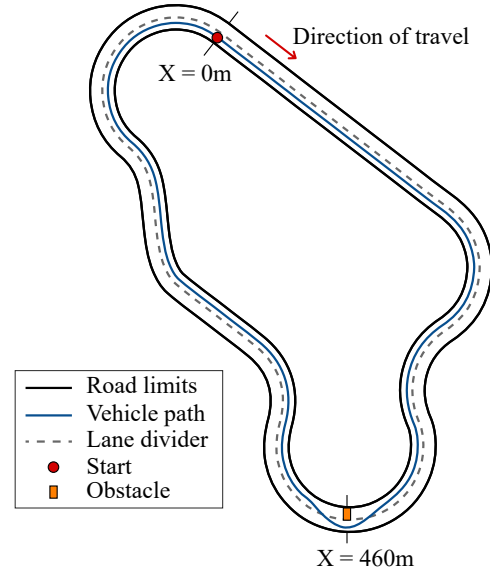

Figure 5. Experimental circuit

Method) to mitigate the learning effect. The collected data includes information such as vehicle states, tire forces and slip angles, the position of the vehicle on the circuit, as well as the steering angle and torque. At the end of the experiment, participants were asked to complete the NASA task load index (TLX) evaluation form to assess the following subjective metrics: *mental demand*, *physical demand*, *performance* and *frustration*. Participants were asked to evaluate each metric on a scale from 1 to 21.

5. Results

The collected data from the runs with and without support of all 32 participants was averaged separately, first per participant and then across all participants of the same category. Statistical significance of the results is assessed using a two-tailed paired t-test, at 5% significance level.

5.1. Objective Evaluation

Figure 6 presents the experimental results as a function of the distance for each of the three driver categories. The first row of plots (plots 6a to 6c) shows the vehicle lateral deviation from the center of the lane. As can be seen, the influence of haptic support on the vehicle path varies for different driver categories. In the case of expert drivers, the haptic support has no noteworthy effect with both trajectories largely overlapping. Novice drivers reduced their peak lateral deviation when driving with the haptic support. A significant change in trajectory is observed in the case of regular drivers. Table 2 presents a comparison of the means of the maximum lateral deviations calculated for each driver category. Regular drivers significantly reduced their peak lateral deviation by 11.28% when driving with haptic support compared to baseline.

The analysis of the averaged root-mean-square (RMS) value of the steering wheel angle in the vicinity of the obstacle, from X=400m to X=550m, is shown in Table 3. The haptic steering support significantly reduced the steering angle for regular and novice drivers, by 16.91% and 25.74% respectively. The difference in steering angle during the experiment can also be observed in Figure 6 (plots 6d to 6f).
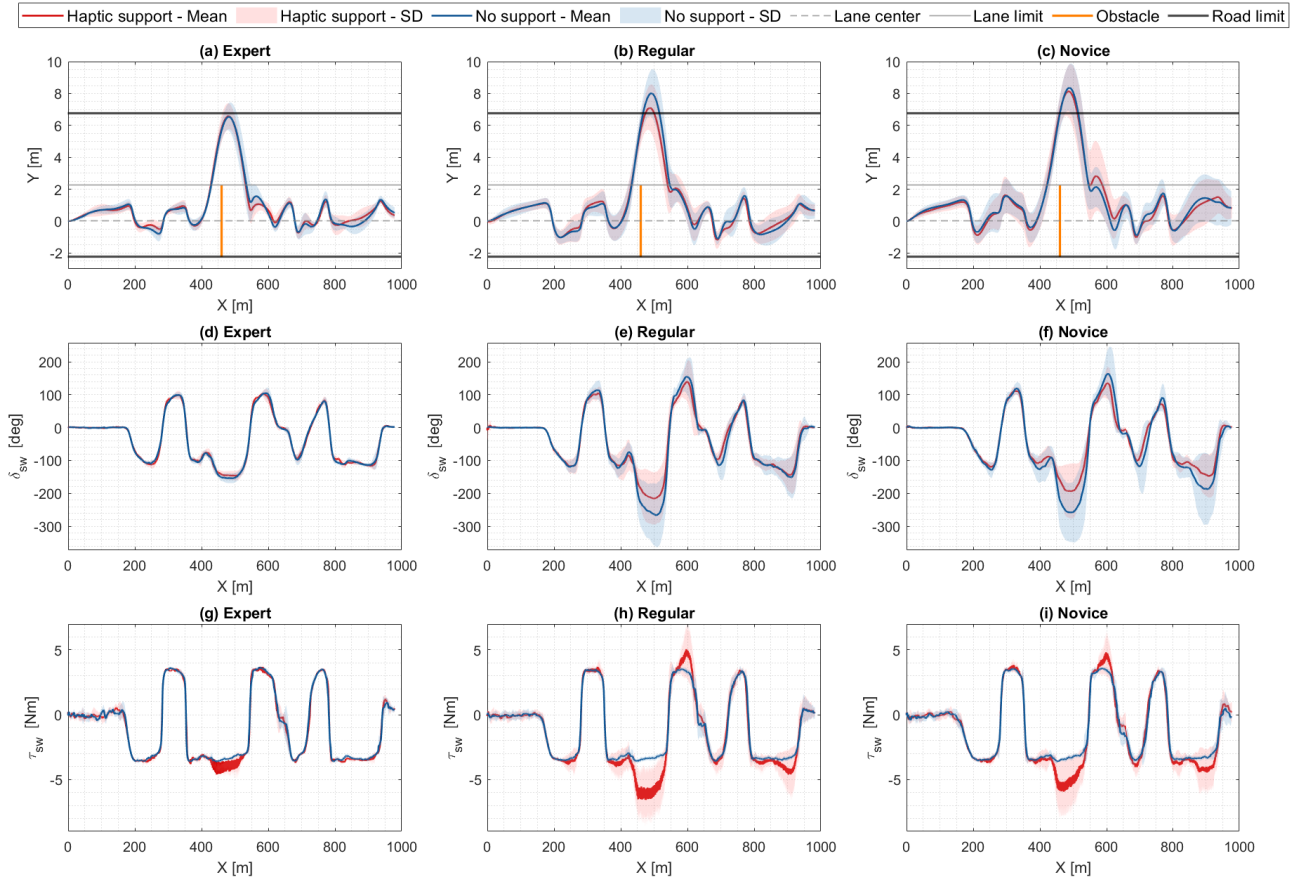
Figure 6. Experimental results: mean values (solid lines), and standard deviations (shaded areas) for the 2 support cases, plotted for each driver group

Drivers	No support	Haptic support	p-value
Expert	6.63m (0.87)	6.60m (0.91)	0.9595
Regular	8.14m (1.51)	7.22m (1.52)	**0.0113**
Novice	8.55m (1.52)	8.30m (1.68)	0.4568

Table 2. Averaged maximum lateral deviation for each driving mode, for each driver category (standard deviations in parentheses)

Drivers	No support	Haptic support	p-value
Expert	125.15° (7.65)	121.28° (8.67)	0.3846
Regular	200.31° (61.33)	166.45° (56.69)	**0.0025**
Novice	195.24° (68.32)	144.99° (46.84)	**0.0077**

Table 3. Averaged RMS values of steering wheel angle from X=400m to X=550m (around the obstacle) for each driving mode, for each driver category (standard deviations in parentheses)

Table 4 presents the RMS values of the total torque on the steering wheel on the interval from X=400m to X=550m. The difference in total steering torque between baseline and proposed system is significant for all categories of drivers, with an increase in torque of 10.23%, 38.83%, and 27.27% for expert, regular, and novice drivers, respectively. This indicates that the haptic support activated on average for all participants, regardless of their driving skills. This is illustrated in Figure 6 (plots 6g to 6i), which shows

an increase in the measured torque on the steering wheel between X=400m and X=550 for all drivers.

Drivers	No support	Haptic support	p-value
Expert	3.24N (0.03)	3.60N (0.30)	**0.0390**
Regular	3.20N (0.07)	4.98N (1.30)	**<0.001**
Novice	3.20N (0.08)	4.39N (1.28)	**0.0095**

Table 4. Averaged RMS values of steering wheel torque from X=400m to X=550m (around the obstacle) for each driving mode, for each driver category (standard deviations in parentheses)

Lastly, the RMS lateral force values for the front axle can be found in Table 5, on the interval from X=400m to X=550m. A significant difference can be noted for regular and novice drivers, who utilised respectively 1.00% and 1.03% additional lateral force during the obstacle avoidance maneuver when driving with haptic support.

5.2. Subjective Evaluation

The averaged results of the NASA-TLX evaluation form are summarized separately for expert, regular and novice driver categories, in Tables 6, 7 and 8, respectively. A significant decrease in mental demand is reported by novice drivers. Regular drivers report a significant increase in self-assessed performance when driving with haptic support. Also, a significant decrease in perceived frustration

Drivers	No support	Haptic support	p-value
Expert	6896.5N (79.14)	6963.3N (101.44)	0.0965
Regular	6737.1N (204.39)	6804.9N (174.14)	**0.0424**
Novice	6758.2N (228.62)	6828.8N (204.15)	**0.0106**

Table 5. Averaged RMS values of lateral force at the front axle from X=400m to X=550m (around the obstacle) for each driving mode, for each driver category (standard deviations in parentheses)

can be observed for novice drivers when aided by haptic support compared to no support.

Metric	No support	Haptic support	p-value
Mental demand	6.80 (5.36)	6.60 (5.13)	0.3739
Physical demand	5.20 (5.02)	6.00 (4.47)	0.3739
Performance	15.40 (2.97)	16.00 (2.65)	0.2080
Frustration	8.6 (6.80)	9.8 (8.70)	0.3883

Table 6. NASA-TLX evaluation results for expert drivers, for each driving mode (standard deviations in parentheses)

Metric	No support	Haptic support	p-value
Mental demand	12.00 (4.50)	11.60 (4.24)	0.6044
Physical demand	9.60 (3.81)	10.07 (4.48)	0.5892
Performance	12.47 (3.56)	14.67 (3.58)	**0.0176**
Frustration	9.33 (4.81)	9.13 (4.75)	0.8003

Table 7. NASA-TLX evaluation results for regular drivers, for each driving mode (standard deviations in parentheses)

After the experiment, participants were also asked about their interest in having the haptic support system in their own personal vehicle, should such technology become available on the market. The results revealed that 3 out of 5 expert drivers are interested in having such a system installed. In the case of regular drivers, a vast majority of 13 out of 15 participants expressed their desire for its implementation. Similarly, among novice drivers, 10 out of 12 participants showed interest in having haptic support installed in their vehicles.

5.3. Discussion

The results show that haptic driver support does impact the drivers, however, the degree to which a driver is influenced greatly depends on their driving skills. Regular drivers seem to particularly benefit from the haptic support, which allows them to deviate significantly less from the road. This is also reflected by the increase in self-assessed performance for regular drivers in the NASA-TLX form. This improvement in performance can be linked to the decrease in steering wheel angle during obstacle avoidance, which allows more lateral force to be generated at the front axle. It should be noted that regular drivers exhibit similarities with expert drivers in terms of steering wheel angle, front axle lateral force and lateral deviation when driving with the haptic support system.

Novice drivers also show a significant reduction in their steering input, along with a significant increase in lateral force on the front

Metric	No support	Haptic support	p-value
Mental demand	14.50 (4.03)	11.58 (5.00)	**0.0431**
Physical demand	12.08 (5.79)	10.67 (4.77)	0.3474
Performance	10.58 (3.94)	11.33 (5.16)	0.6975
Frustration	11.58 (4.56)	8.33 (4.33)	**0.0310**

Table 8. NASA-TLX evaluation results for novice drivers, for each driving mode (standard deviations in parentheses)

axle. However, no significant decrease in lane deviation is noticed. More research is needed in this area, however, factors like reaction time and how early a driver starts the evasive maneuver could be of importance. Nevertheless, novice drivers scored significantly lower on the reported frustration metric and mental demand. Hence, the proposed system also has a positive influence on less experienced drivers and can help reduce the perceived workload during an emergency maneuver.

Lastly, no significant differences can be found for expert drivers in terms of objective or subjective metrics other than the total measured torque on the steering wheel. While driving with both controller variations, expert drivers outperformed all the other drivers in terms of minimizing lane deviation. On average, they generated the largest lateral force at the front axle while using the smallest steering input to perform the evasive maneuver. Furthermore, they scored the lowest on both mental and physical demand metrics. Therefore, haptic support systems have no significant influence on expert drivers, who can reliably assess the situation by themselves. In fact, haptic support could be the linked with a slight increase in frustration reported by expert drivers, however the difference is not statistically significant. More research should be done on identifying relevant differences between expert and regular/novice drivers in emergency scenarios that could be linked with safer maneuvers.

6. Conclusion and Future Work

In this study, a predictive haptic driver support system was proposed with the aim of mitigating vehicle understeer. The system operates by intuitively alerting the driver about incoming front tire saturation limits in advance. In order to validate the system, a driving simulator study was performed involving an obstacle avoidance maneuver in the middle of a turn. Results demonstrate that haptic support has a positive impact on regular drivers' behavior, characterized by a reduced RMS steering angle value compared to manual steering. This results in higher lateral force at the front axle which translates to a smaller lateral deviation from the lane. The proposed system also positively influenced novice drivers in reducing their steering input during the maneuver, and significantly increased the lateral force at the front tires. However, no significant decrease in lane deviation has been observed for novice drivers. Subjective evaluation indicates a significant increase in self-assessed performance for regular drivers who drove with haptic support. Similarly, novice drivers report significantly reduced mental demand and frustration when haptic support is active. Expert drivers are the least affected by the haptic support system and show no significant difference in performance or reported subjective metrics.

Future research focuses on adapting the proposed haptic driver support to scenarios with varying vehicle speeds. The system could be extended to provide support in adjusting the speed and the steering input at the same time with integrated vehicle control. The combination of the haptic driver support with differential braking offers an interesting direction for further investigation.

References

[1] M. Kyriakidis, C. van de Weijer, B. van Arem, and R. Happee. "The deployment of Advanced Driver Assistance Systems in Europe". In: *Proceedings of 22nd ITS World Congress, Bordeaux, France*. 2015.

[2] R. Elvik. "International transferability of accident modification functions for horizontal curves". In: *Accident Analysis & Prevention* 59 (2013), pp. 487–496.

[3] M. Klomp, M. Lidberg, and T. Gordon. "On optimal recovery from terminal understeer". In: *Proceedings of the Institution of Mechanical Engineers, Part D: Journal of Automobile Engineering* 228.4 (2014), pp. 412–425.

[4] S. Othman, R. Thomson, and G. Lannér. "Identifying critical road geometry parameters affecting crash rate and crash type". In: *Annals of advances in automotive medicine/annual scientific conference*. Vol. 53. 2009, pp. 155–165.

[5] T. Gordon, M. Klomp, and M. Lidberg. "Strategies for Minimizing Maximum Off-tracking resulting from Over-speed in Curves". In: *Proceedings of 11th International Symposium on Advanced Vehicle Control, Seoul, South Korea*. 2012.

[6] Y. Gao and T. Gordon. "Optimal control of vehicle dynamics for the prevention of road departure on curved roads". In: *IEEE Transactions on Vehicular Technology* 68.10 (2019), pp. 9370–9384.

[7] V. Fors, B. Olofsson, and L. Nielsen. "Yaw-moment control at-the-limit of friction using individual front-wheel steering and four-wheel braking". In: *IFAC-PapersOnLine* 52.5 (2019), pp. 458–464.

[8] A. Lazcano, T. Niu, X. Akutain, D. Cole, and B. Shyrokau. "MPC-based haptic shared steering system: A driver modeling approach for symbiotic driving". In: *IEEE/ASME Transactions on Mechatronics* 26.3 (2021), pp. 1201–1211.

[9] J. Takahashi, M. Yamakado, S. Saito, and A. Yokoyama. "A hybrid stability-control system: combining direct-yaw-moment control and G-Vectoring Control". In: *Vehicle system dynamics* 50.6 (2012), pp. 847–859.

[10] M. Yamakado and M. Abe. "An experimentally confirmed driver longitudinal acceleration control model combined with vehicle lateral motion". In: *Vehicle System Dynamics* 46.S1 (2008), pp. 129–149.

[11] D. Abbink, T. Carlson, M. Mulder, J. De Winter, F. Aminravan, T. Gibo, and E. Boer. "A topology of shared control systems—finding common ground in diversity". In: *IEEE Transactions on Human-Machine Systems* 48.5 (2018), pp. 509–525.

[12] D. Katzourakis. "Driver steering support interfaces near the vehicle's handling limits". PhD dissertation, Faculty of Mechanical, Maritime and Materials Engineering, Delft University of Technology, 2012.

[13] J. Van Doornik. "Haptic feedback on the steering wheel near the vehicle's handling limits using wheel load sensing". MSc thesis, Faculty of Mechanical, Maritime and Materials Engineering, Delft University of Technology, 2014.

[14] Stijn Kerst, Barys Shyrokau, and Edward Holweg. "A model-based approach for the estimation of bearing forces and moments using outer ring deformation". In: *IEEE Transactions on Industrial Electronics* 67.1 (2019), pp. 461–470.

[15] H. B. Pacejka. *Tire and Vehicle Dynamics, 3rd ed.* Oxford, U.K.: Butterworth-Heinemann, 2012.

[16] C. Hildebrandt, M. Schmidt, M. Sedlmayr, O. Pion, G. Büyükyildiz, and F. Küçükay. "Intuitive steering assistance in critical understeer situations". In: *Traffic injury prevention* 16.5 (2015), pp. 484–490.

[17] R. Rajamani. *Vehicle dynamics and control*. Springer Science & Business Media, 2011.

[18] E. Fiala. "Lateral forces on rolling pneumatic tires". In: *Zeitschrift VDI* 96.29 (1954), pp. 973–979.

[19] C. E. Beal and J.C. Gerdes. "Model predictive control for vehicle stabilization at the limits of handling". In: *IEEE Transactions on Control Systems Technology* 21.4 (2012), pp. 1258–1269.

[20] A. Domahidi and J. Jerez. *FORCES Professional*. Embotech AG, url=https://embotech.com/FORCES-Pro. 2014–2019.

[21] A. Zanelli, A. Domahidi, J. Jerez, and M. Morari. "FORCES NLP: an efficient implementation of interior-point methods for multistage nonlinear nonconvex programs". In: *International Journal of Control* (2017), pp. 1–17.

[22] Mircea Damian, Barys Shyrokau, Xabier Carrera Akutain, and Riender Happee. "Experimental validation of torque-based control for realistic handwheel haptics in driving simulators". In: *IEEE Transactions on Vehicular Technology* 71.1 (2021), pp. 196–209.

[23] S. Othman, R. Thomson, and G. Lannér. "Are driving and overtaking on right curves more dangerous than on left curves?" In: *Annals of Advances in Automotive Medicine/Annual Scientific Conference*. Vol. 54. 2010, pp. 253–264.